Bulletin of the JSME, Vol. 22, No. 170, August 1979

536.423.1:532.595:621.18

Paper No. 170-10

Flow Instabilities in Boiling Channels*

Part 1 Pressure Drop Oscillation

By Mamoru OZAWA**, Shigeyasu NAKANISHI***, Seikan ISHIGAI†,

Yuhsuke MIZUTA†† and Hiroaki TARUI†††

The pressure drop oscillation in a boiling channel system was analyzed by using a lumped parameter model in which the pressure drop characteristics was described by a third order equation of the flow rate. The momentum equation in the boiling channel system was thus reduced to a Van der Pol equation. The limit cycle and the period of the pressure drop oscillation obtained from the Van der Pol equation agreed qualitatively with experimental results.

1. Introduction

Increasing attention has been given to the flow instability in steam generators with the development of the Liquid Metal Fast Breeder Reactor because of its severe operational and safety problems caused by the flow instability. There have been many analytical and experimental investigations on the flow instability as can be found in the review paper by Bouré et al.[1] But not all the aspects associated with the flow instability are fully understood.

We have already reported the experimental and the analytical investigations on the density wave oscillation,[2,3] which is the most common phenomenon encountered in the steam generator. This paper presents the experimental and analytical results on the pressure drop oscillation, which is one of the typical nonlinear oscillations in a boiling channel system.

The pressure drop oscillation will occur in a system with a sufficient compressible volume upstream of the boiling channel, when the pressure drop across the channel decreases with an increase in the flow rate.

Maulbetsch et al.[4] and Stenning et al.[5,6] have shown that the pressure drop oscillation is caused by the dynamic interaction between the compressible volume and the channel, that the period and the amplitude of the oscillation are much larger than those of the density wave oscillation, and that the period depends mainly on the upstream compressible volume. Since their analyses have not taken into account the nonlinearity of the pressure drop vs. flow rate characteristics, the limit cycle of the pressure drop oscillation has not been obtained. Though a numerical analysis[7] is available to obtain the limit cycle of the pressure drop oscillation, it is not suitable for the understanding of the general feature of the oscillation. In this paper, the pressure drop oscillation is analyzed by using a lumped parameter nonlinear model of the boiling channel system in order to investigate the effect of the various parameters on the limit cycle of the oscillation. The analytical results of the limit cycle and the period of the pressure drop oscillation are compared with the experimental results.

Notations

A, A', A_s, A_s'	: cross sectional areas
L, L', L_s, L_s'	: lengths
G, G_o, G_s	: mass flow rates
P, P_o, P_s	: pressures
t	: time
ρ_f	: density of the liquid
κ	: specific heat ratio
g	: gravitational acceleration
q	: heat flux density
T_{in}	: fluid temperature at the inlet
T_s	: saturation temperature
$\Delta T_{sub} = T_s - T_{in}$	
τ	: period of the oscillation
ΔP_v	: pressure drop at the Venturi flowmeter
ΔP_t	: pressure drop across the boiling channel

2. Experimental apparatus and experimental procedure

The experimental apparatus used in this study is a forced flow boiling loop designed for R-113, which is suitable for this experiment because of its low saturation temperature and low latent heat of vaporization. Figure 1 is a schematic diagram of the boiling loop. The principal parts of the boiling loop are a liquid tank, a diaphragm pump, a preheater, a test section, a drum, a condenser, a subcooler and a surge tank. The test section is a vertical SUS304 tube, 3.84 mm I.D., 6.0 mm O.D. and 2.68 m heated length. It is heated directly by AC power.

* Received 4th April, 1977.

** Research Associate, Faculty of Engineering, Osaka University, Suita.
*** Associate Professor, Faculty of Engineering, Osaka University, Suita.
† Professor, Faculty of Engineering, Osaka University, Suita.
†† Engineer, Prefectural Office, Fukui.
††† Engineer, Sumitomo Metal Industries Ltd., Amagasaki.

Because of the constant wall thickness of the tube, the heat flux density is essentially uniform. The surge tank is a cylindrical vessel with 105 mm I.D. and 2 m height and contains N_2 gas. A sight section is installed in the riser section downstream of the test section to permit visual observation of the flow in the riser section. In this experiment the bypass valve V_5 is always closed.

The flow rate is controlled by adjusting the pump speed, the pump stroke and the openings of the valves V_1 and V_2, and is measured by the orifice flowmeter and the Venturi flowmeter. The pressure drops at the Venturi flowmeter and the test section are measured by the D.P. cells and the strain amplifiers and are recorded by the pen recorder. The temperature at the inlet of the test section is controlled by adjusting the power input to the preheater. Sheathed thermocouples of 1.6 mm diameter and a digital voltmeter are used to measure the fluid temperatures. The wall temperature of the test section is measured by C-A thermocouples of 0.3 mm diameter. The drum pressure which is referred to as the system pressure is controlled by adjusting the water flow to the condenser, and is determined as the saturated vapor pressure for the fluid temperature in the drum. Other pressures throughout the loop are measured by Bourdon tube pressure gauges. The power inputs to the test section are measured by a wattmeter. The test section, the preheater and the drum are insulated by glasswool in order to decrease the heat loss.

The experimental procedure is as follows: The test section is isolated from the surge tank by the valve V_3, and then the drum pressure, the inlet temperature, the power input and the flow rate are brought to a predetermined steady state. After measuring the various parameters at the steady state, the valve V_3 is opened gradually. Sufficient time is allowed so that the steady pressure drop oscillation can be observed.

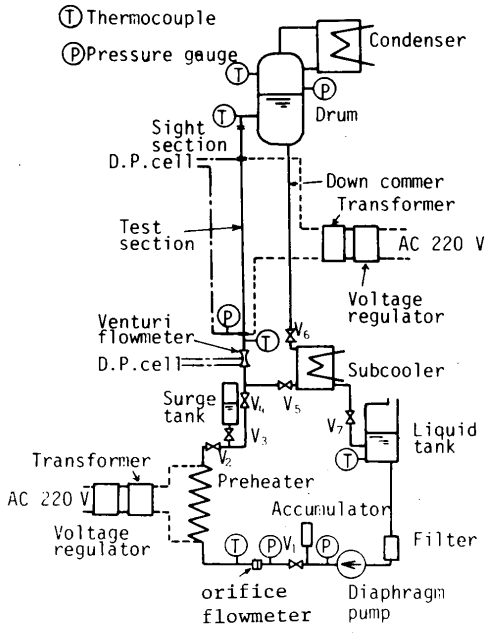

Fig.1 Experimental apparatus

3. Experimental results

Figure 2 shows the typical traces of the pressure drop at the Venturi flowmeter (corresponding to the inlet flow rate) and the pressure drop across the test section. The pressure drop at the Venturi flowmeter ΔP_v increases rapidly during the state (A) to (B), then decreases during the state (B) to (D). On the other hand, the pressure drop across the test section ΔP_t increases during the states (C)-(D)-(A), and decreases during the states (A)-(B)-(C). At the state (D), the pressure drop ΔP_v has a minimum value and begins to oscillate with high frequency. As ΔP_v increases gradually during the states (D) to (A), the high frequency oscillation is damped. At some experimental conditions a burn-out may occur at the test section during the states (D) to (A). The high frequency oscillation and the burn-out depend entirely upon the experimental range, and are not essential features of the pressure drop oscillation. The low frequency oscillation (corresponding to the states (A)-(B)-(C)-(D)-(A)) is a pressure drop oscillation.

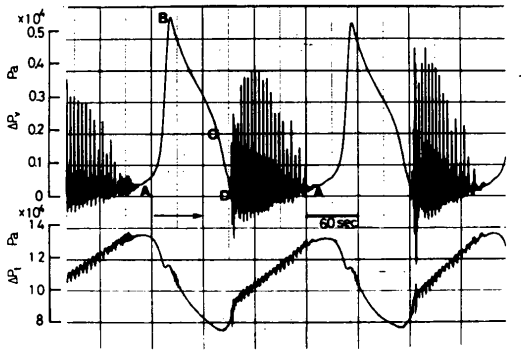

P = 2.17×10^5 Pa q = 3.59×10^4 W/m
ΔT_{sub} =47.8 K G =60.5 kg/h V_s =3.6×10^{-3} m^3

Fig.2 Typical trace of the oscillation

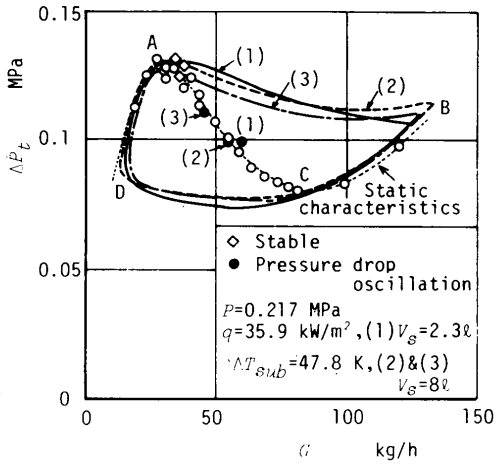

Fig.3 Limit cycle

The pressure drop vs. flow rate characteristics of the test section is shown in Fig.3. The characteristics involve the region where the pressure drop decreases with an increase in the flow rate, i.e. the negative slope region. In Fig.3, the limit cycles of the pressure drop oscillation are also shown. The limit cycle shows the relation between the pressure drop and the flow rate during the oscillation. The limit cycles (1), (2) and (3) are obtained under the condition corresponding to the equilibrium states (1), (2) and (3) respectively. The states (A), (B), (C) and (D) in Fig.3 correspond to the states (A), (B), (C) and (D) in Fig.2 respectively. The limit cycles on the pressure drop vs. flow rate plane almost coincide with each other, while the experimental conditions, i.e. the compressible volume in the surge tank and the flow rate at the equilibrium state, are different in these limit cycles. The limit cycle curves from (D) to (A) and from (B) to (C) almost coincide with the static characteristics of the pressure drop across the test section.

4. Analysis

4.1 Analytical model

Maulbetsch et al.[4] and Stenning et al[5,6] have already investigated the mechanism of the pressure drop oscillation: The necessary conditions for the occurrence of the pressure drop oscillation are that the operating condition be in the negative slope region of the pressure drop vs. flow rate characteristics and that the system have an energy storage mechanism such as the upstream compressible volume. However, very long boiling channels may suffer from the pressure drop oscillation due to the compressibility inherent in the boiling channel itself.

In Fig.4 an analytical model of the boiling channel system is shown. The model consists of a feeder section, a heated section and a surge tank upstream of the boiling channel. The surge tank is connected to the feeder section by a tube with the cross sectional area A_S' and the length L_S'. The surge tank contains compressible gas and the liquid level in the tank is L_S. This model is similar to the models of Maulbetsch et al.[4] and Stenning et al[5,6], but is different in that the restrictions at the inlet of the surge tank and the boiling channel are ignored in this model. These restrictions, not being essential for the pressure drop oscillation, are neglected for simplicity.

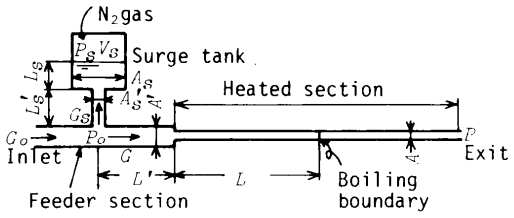

Fig.4 Model of the boiling channel system

4.2 Analysis

As the pressure drop oscillation is a typical nonlinear oscillation, it is necessary to take into account the nonlinear characteristics of the pressure drop in order to obtain the limit cycle of the oscillation. In this paper, the pressure drop characteristics across the boiling channel is approximated by a third order equation of the flow rate.

In order to prepare the mathematical representations of the dynamic behaviour of the boiling channel system with the upstream compressible volume, it is necessary to make assumptions:

(1) The inflow to the system G_o is constant.
(2) The exit pressure of the boiling channel P is constant.
(3) The acceleration of the flow due to vaporization is not taken into account.
(4) The mass of the liquid in the boiling region is small compared with that in the subcooled liquid region and is ignored for simplicity.
(5) The masses of the liquid in the feeder section, in the subcooled liquid region and in the surge tank are assumed to be constant during the oscillation and equal to the values at the equilibrium state respectively.

Using thses assumptions and the notations of Fig.4, the following equations of motion can be written

$$P_0-P_i=I_i\frac{dG_i}{dt} \quad \cdots\cdots(1)$$

$$P_0-P=f(G)+I\frac{dG}{dt} \quad \cdots\cdots(2)$$

where $I_i=L_i/A_i+L_i'/A_i'$, $I=L/A+L'/A'$

which are considered to be constant from the assumption (5), and the function $f(G)$ represents the pressure drop across the boiling channel. This function $f(G)$ has a maximum value at the flow rate G_a and a minimum value at the flow rate G_b, and the derivative $df(G)/dG$ is negative within the range $G_a < G < G_b$. Then the derivative can be written as

$$\frac{df(G)}{dG}=\alpha(G-G_a)(G-G_b) \quad \cdots\cdots(3)$$

where α is a positive constant.

The variation of compressible gas volume in the surge tank due to the inflow G_S to the surge tank is represented by

$$G_i=-\rho_f\frac{dV_i}{dt} \quad \cdots\cdots(4)$$

If the state of the gas in the surge tank changes adiabatically, the relation between the pressure P_S and the gas volume V_S in the surge tank can be represented by $P_S \cdot V_S^K$ = constant, then Eq.(4) becomes

$$G_i=C_i\frac{dP_i}{dt} \quad \cdots\cdots(5)$$

where $C_i=\rho_f V_i/(\kappa P_i)$

and C_S is constant during the oscillation. The values of P_S and V_S are determined from the equilibrium state.

A differentiation of Eqs.(1) and (2) with respect to time gives

$$\frac{dP_0}{dt}-\frac{dP_s}{dt}=I_s\frac{d^2G_s}{dt^2} \quad \cdots\cdots(6)$$

$$\frac{dP_0}{dt}=\frac{df(G)}{dG}\frac{dG}{dt}+I\frac{d^2G}{dt^2} \quad \cdots\cdots(7)$$

Eliminating dP_S/dt and dP_o/dt from Eqs.(5), (6) and (7), we obtain

$$(I+I_s)\frac{d^2G}{dt^2}+\frac{df(G)}{dG}\frac{dG}{dt}-\frac{G_s}{C_s}=0 \quad \cdots\cdots(8)$$

As the inflow to the system G_o is the sum of the inflow to the surge tank G_S and the inflow to the boiling channel G, i.e. $G_o=G_S+G$, Eq.(8) becomes

$$(I+I_s)\frac{d^2G}{dt^2}+\frac{df(G)}{dG}\frac{dG}{dt}+\frac{G-G_0}{C_s}=0 \quad \cdots\cdots(9)$$

We now introduce the dimensionless parameters

$$G^*=\frac{G-G_0}{G_0}, \quad t^*=\frac{t}{\sqrt{C_s(I+I_s)}} \quad \cdots\cdots(10)$$

Substituting Eq.(10) into Eqs.(3) and (9) and eliminating $df(G)/dG$ from Eqs.(3) and (9), we obtain

$$\frac{d^2G^*}{dt^{*2}}-\sqrt{\frac{C_s}{I+I_s}}\alpha G_0^2G_a^*G_b^*\left(1-\frac{G_a^*-G_b^*}{G_a^*G_b^*}G^*-\frac{G^{*2}}{G_a^*G_b^*}\right)\frac{dG^*}{dt^*}+G^*=0 \quad \cdots\cdots(11)$$

where $G_a^*=(G_0-G_a)/G_0$, and $G_b^*=(G_b-G_0)/G_0$

Another dimensionless parameter is introduced as follows:

$$G^*=\sqrt{G_a^*G_b^*}y^* \quad \cdots\cdots(12)$$

The substitution of Eq.(12) into Eq.(11) gives

$$\frac{d^2y^*}{dt^{*2}}-\varepsilon(1-2\beta y^*-y^{*2})\frac{dy^*}{dt^*}+y^*=0 \quad \cdots\cdots(13)$$

where ε and β are dimensionless parameters and are written as follows:

$$\varepsilon=\sqrt{\frac{C_s}{I+I_s}}\alpha G_0^2G_a^*G_b^*, \quad \beta=\frac{G_a^*-G_b^*}{2\sqrt{G_a^*G_b^*}} \quad \cdots\cdots(14)$$

In case of $\beta=0$ the equation (13) is a well-known Van der Pol equation. Thus the momentum equation in the boiling channel system with the upstream compressible volume is reduced to Eq. (13). The limit cycle of the pressure drop oscillation can be determined uniquely by the dimensionless parameters ε and β, which are calculated from the equilibrium values of the flow rate, the gas volume in the surge tank, the mass of the liquid and the static characteristics of the pressure drop across the boiling channel.

4.3 Comparison between the analytical results and the experimental results

The equation (13) is solved by the method of isoclines in order to obtain the limit cycle on the dy^*/dt^* - y^* plane. The integration

$$t^*=\int\frac{1}{(dy^*/dt^*)}dy^* \quad \cdots\cdots(15)$$

is carried out graphically along the limit cycle to give y^* - t^* curve, i.e. $(G-G_o)/G_o$ - t curve and dG/dt - t curve. From these curves and Eq.(2) the pressure drop vs. time can be obtained.

Now we must show the existence of a solution of Eq.(15) in the neighbourhood of $dy^*/dt^*=0$ on the limit cycle. Then the dimensionless parameters are, for instance, $\varepsilon=7.77$, $\beta=-1.35$, the limit cycle in the region of $dy^*/dt^*<0$ and in the neighbourhood of $dy^*/dt^*=0$ can be approximated by the following equations

$$\frac{dy^*}{dt^*}=-0.25(4.6-y^*)^{1/2} \qquad 4.5\leqq y^*\leqq 4.6 \qquad (16)$$

and

$$\frac{dy^*}{dt^*}=-15.0(2.0+y^*)^{1/2} \qquad -2.0\leqq y^*\leqq -1.9 \qquad (17)$$

Substituting Eqs.(16) and (17) into Eq.(15), we obtain

$$t^*=4(4.6-y^*)^{1/2} \qquad 4.5\leqq y^*\leqq 4.6 \qquad (18)$$

and

$$t^*=(2+y^*)^{1/2}/15.0+t_0^* \qquad -2.0\leqq y^*\leqq -1.9 \qquad (19)$$

This shows the existence of a soultion of Eq.(15) in the neighbourhood of $dy^*/dt^*=0$. In cases of the derivative $dy^*/dt^*>0$ and the other values of ε and β, the existence of a solution of Eq.(15) can be proved in the same manner as described above. Thus, there is no problem in the graphical integration of Eq. (15).

In Fig.5, the solid line shows the static characteristics of pressure drop vs. flow rate in the boiling channel. This curve is obtained by the numerical integration of the correlations of Lockhart and Martinelli[8] In this figure, the approximate curve of the pressure drop obtained from Eq.(3) is also shown by a dot-dash-line, and the constant α is chosen such that the approximate curve coincides with the curve obtained by the numerical integration in the negative slope region. The values of G_a and G_b depend on the operating parameters, such as the pressure, the heat flux and the inlet subcooling, and G_a = 40 kg/h, G_b = 95 kg/h in this example. Two limit cycles of the pressure drop oscillation obtained from Eq.(13) are also shown in the figure, and the corresponding equilibrium states are represented by the marks o and ●. The state travels on the limit cycles

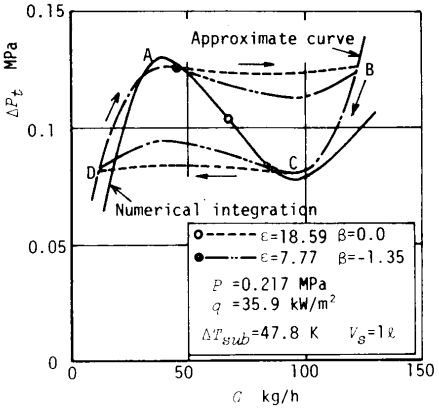

Fig.5 Limit cycle

in the direction represented by the arrows, and almost coincides with the approximate static characteristics of the pressure drop in between the states (D)-(A) and (B)-(C). This fact agrees with the experimental results. The limit cycles during the states (A)-(B) and (C)-(D) are different from each other for different values of ε and β .

In Figs.(6) and (7) the oscillations of the pressure drop and the flow rate obtained from the analysis are compared with those of the experimental results. In these figures the time axis t is normalized by the period τ . The analytical results agree with the experimental results. In these examples, the dimensionless parameter β is negative, so the portion of $G < G_o$ in one wave length is longer than that of $G > G_o$. In the contrary cases of $\beta > 0$, the portion of $G > G_o$ in one wave length become longer than that of $G < G_o$. This is due to the characteristics of Eq.(13). Figure (8) shows the relation between the oscillation period τ and the compressible volume in the surge tank V_s. The experimental results increase linearly with an increase in the gas volume V_s. The analytical results agree qualitatively with the experimental results, and are 40 % less than the experimental ones. An increase in the compressible volume results in an increase in the dimensionless parameter ε , which in turn elongates the oscillation period. This is also the characteristics of Eq.(13).

The quantitative disagreement between the analytical results and the experimental ones of the oscillation period is probably due to the assumption that the parameters C_s , I and I_s are constant during the oscillation, partly to the poor fit of the approximate pressure drop characteristics, and partly to the fact that this model does not take into account the compressibility in the boiling region and the restriction at the surge tank inlet. In estimating the effects of these factors on the oscillation, the numerical calculation with a digital computer by such method as the finite difference method will be available.

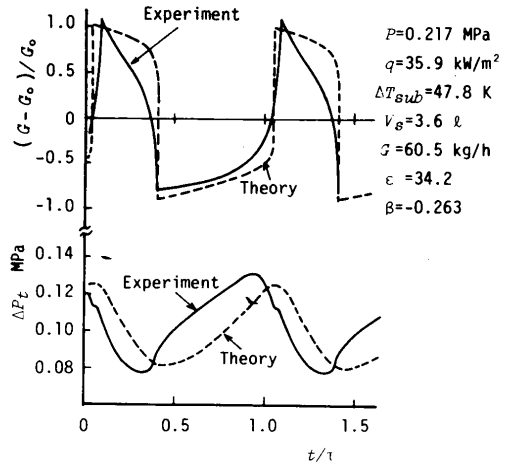

Fig.6 Oscillations of flow rate and pressure drop

5. Conclusions

An experimental study on the pressure drop oscillation is conducted by using a boiling channel system with the upstream compressible volume. The pressure drop oscillation is analyzed by using a lumped parameter nonlinear model. The conclusions of this study may be summarized as follows:
(1) The momentum equation in the boiling channel system is reduced to a Van der Pol equation by using the lumped parameter nonlinear model, in which the pressure drop characteristics is described by a third order equation of the flow rate.
(2) The effect of the operating conditions on the pressure drop oscillation can be understood by two dimensionless parameters ε and β .
(3) The limit cycles and the oscillation periods obtained from the analysis agree qualitatively with the experimental results.

Authors wish to thank Yoshitsugu Kasai, Tadayoshi Matsumoto, Kenji Tokunaga and Tetsuo Nakazato for their assistance in carrying out the experimental part of this work. A part of this experiment was supported by Hitachi Ltd., Babcock Hitachi Co. Ltd., and Kawasaki Heavy Industry Co. Ltd.

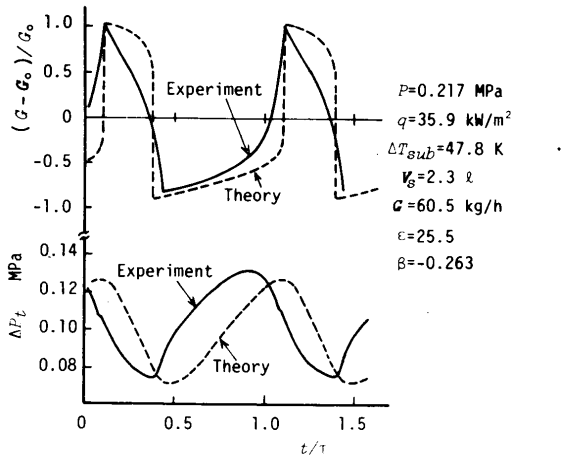

Fig.7 Oscillations of flow rate and pressure drop

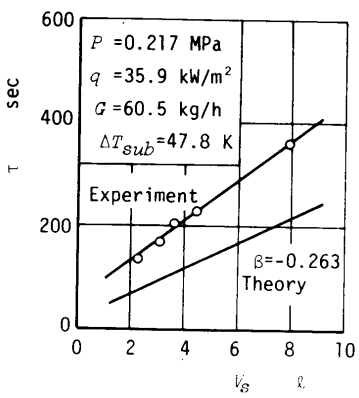

Fig.8 Oscillation period

References

1) Bouré, J.A., et al., ASME Paper 71-HT-42 (1971), 1.
2) Nakanishi, S., et al., Theoretical and Applied Mechanics, Vol.26(1978), 421.
3) Nakanishi, S., et al., Technology reports of the Osaka Univ., Vol.28, No.1421(1978), 243.
4) Maulbetsch, J.S., Griffith, P., 3rd International Heat Transfer Conference, Shicago (1966), 247.
5) Stenning, A.H., Veziroglu, U.N., Proc. 1965 Heat Transfer and Fluid Mechanic Institute(1965), 301, Stanford Press.
6) Stenning, A.H., et al., EURATOM Report, Proc. Symp. on Two-Phase Flow Dynamics, Eindhoven(1967), 405.
7) Nariai, H., et al., 13th Annual Symp. Heat Transfer Society of Japan, Kobe (1976), 490.
8) Lockhart, R.W., Mantinelli, R.C., Chem. Eng. Prog., 45-1(1949), 39.